

Design a cabinet dryer with two geometric configurations using CFD

H. Darabi · A. Zomorodian · M. H. Akbari ·
A. N. Lorestani

Revised: 13 March 2013 / Accepted: 20 March 2013 / Published online: 19 April 2013
© Association of Food Scientists & Technologists (India) 2013

Abstract Cabinet dryers are the most popular devices for fruit drying. One of the drawback of this dryer can be non-uniformity in the desired end product moisture content. To surmount this problem, a new version of cabinet dryer with separate entrances for the trays was designed in this research. Some involving physical properties of fruit such as air flow resistance, kernel and bulk densities and porosity were measured. Several different three dimensional geometries of cabinet dryer with three fruit holding trays were studied theoretically using Computational Fluid Dynamics (CFD) technique. The most appropriate geometrical sketch with acceptable uniform air flow and temperature distribution in the cabinet dryer was selected and fabricated. Several experiments were conducted on the new pilot size dryer Lemon fruit with initial moisture content of 84 % (wb) was selected to be dried in the new dryer. The experimental results showed that the new cabinet dryer illustrated an even distribution of air velocity and temperature throughout the dryer. Comparing the experimental and predicted (extracted for the CFD analysis) data under different operating conditions (air velocities of 1, 2 and 3 ms⁻¹, initial product

moisture content of 84 %(wb) and drying air temperature of 50 °C) revealed a very good correlation coefficient of 0.99 for air velocity in the drying chamber. In the next step, the new cabinet dryer was compared with the existing design Amanlou and Zomorodian (J Food Eng 101: 8–15, 2011) with air flow distribution uniformity among the trays, rate of drying in different trays, and electrical energy consumptions, It was revealed that the new design was superior to the existing design in all of these aspects.

Keywords Lemon fruit · Cabinet drying · Numerical and experimental investigation

Nomenclature

C, D	prescribed matrices
$C_0; C_1$	empirical coefficients
C_{ij}	prescribed matrices
D_{ij}	mass diffusion coefficient
ρ	density of fluid
k	turbulent kinetic energy
ε	rate of dissipation
μ	dynamic viscosity
μ_t	turbulent viscosity
G_k	generation of turbulent kinetic energy due to the mean velocity gradients
G_b	generation of turbulent kinetic energy due to buoyancy
Y_M	contribution of the fluctuating dilatation in compressible turbulence to the overall dissipation rate
$C_{1\varepsilon}, C_{2\varepsilon}, C_{3\varepsilon}$	constants used in turbulent model
σ_k	turbulent Prandtl numbers for k
σ_ε	turbulent Prandtl numbers for ε
E	total energy
\mathbf{u}_i	velocity vector
u_{mag}	velocity magnitude
$(\tau_{ij})_{eff}$	deviatoric stress tensor

H. Darabi (✉)
Department of agricultural engineering, Faculty of agriculture,
Shiraz University, Shiraz, Iran
e-mail: darabyhamed@yahoo.com

A. Zomorodian
Department of agricultural engineering, Faculty of agriculture,
Shiraz University, Shiraz, Iran
e-mail: azomoro@shirazu.ac.ir

M. H. Akbari
Department of mechanical engineering, Shiraz University,
Shiraz, Iran
e-mail: h_akbari@shirazu.ac.ir

A. N. Lorestani
Mechanical Engineering of Agricultural Machinery Department,
Faculty of Agriculture, Razi University, Kermanshah, Iran
e-mail: ali.lorestani@gmail.com

P	pressure
Pr_t	Prandtl number
T	temperature
c_p	specific heat capacity at constant pressure
u	velocity magnitude in x direction
t	time
S_k, S_ε, S_h	user-defined source terms
S_i	source term for i th momentum equation

Introduction

Cabinet dryers are the most favorite equipment used in farms for fruit drying. These dryers are simple in structure, low in cost installation and can be employed in almost any environmental conditions. Non-uniformity in the moisture content of the end product is an inherent drawback in applying the cabinet dryer; hence producers are not usually interested in utilizing this drying system (Adams and Thompson 1985; Mathioulakis et al. 1998; Mirade 2003).

In conventional cabinet dryers, hot air is normally introduced under first tray (bottom tray) and passes through the other trays. Therefore the drying materials on the bottom trays would receive the highest energy and might be over dried, while the materials on the other trays may not receive enough energy to be dried due to decrease in drying air potentials. Dehydration rate illustrates a very strong relationship with drying air temperature and velocity (Mulet et al. 1987; Karathanos and Belessiotis 1997).

Uniform air flow distribution inside drying compartment is of paramount importance because it determines both the efficiency and the homogeneity of the products being dried (Mirade 2003). Controlling all of these effective parameters experimentally is a very tedious and difficult task. Although Computational Fluid Dynamics technique (CFD) can not replace physical experiments completely but it can significantly reduce the amount of time needed for experimental works. This valuable tool is capable of analyzing the flow pattern of the air conditioning system in short span of time, which was previously impossible from experimental and theoretical methods (Anderson 1995; Yongson, et al. 2007).

Computational fluid dynamics (CFD) have been extensively applied for predicting the air velocity and temperature profiles in drying chambers (Norton and Sun 2006). With the development of low cost, powerful computers, and commercial software packages such as Fluent, Star-CD and CFX in last decade, CFD has been increasingly deployed in the food industry (Scott and Richardson 1997; Verboven, et al. 2000a, b; Xia and Sun 2002). CFD has been effectively used to study odors dispersion. CFD can consider various atmospheric phenomena and topographical condition to study the occurrence

of odours and aerosol dispersions (Hong et al. 2011). CFD simulation of the four commercial models of corrugated cellulose evaporative cooling pads that are most widely used in Mediterranean greenhouses (A. Franco, et al. 2011). CFD to evaluate the climate distribution in animals body and livestock thermal environment (Norton et al. 2010). Accuracy of prediction can be strongly improved by including some pertinent physical properties of fruits such as: air flow resistance, kernel and bulk densities and porosity in the study (Fluent 6.3 user's Guide 2005). A new cabinet dryer with a side mounted plenum chamber was designed using CFD, constructed and evaluated by Amanlou and Zomorodian 2010. Their experiments were conducted on the most appropriate sketch with acceptable uniform air flow and temperature distribution. Comparing the experimental and predicted (extracted for the CFD analysis) data revealed a very good correlation coefficient of 0.99 and 0.86 for drying air temperature and air velocity in the drying chamber, respectively.

The present research was devoted to design a new version of fruit cabinet dryer with a common side plenum chamber but different air flow entrances beneath the screens holding the drying materials. In this work CFD was employed. The main objectives of this study were the following:

- design a new configuration of cabinet dryer using three dimensional CFD techniques to find the drying air flow and temperature distribution profiles through the drying compartment under and over the screens.
- comparison new cabinet dryer with cabinet dryer amanlou and zomorodian designed with air flow distribution uniformity among the trays, rate of drying in different trays, and electrical energy consumptions.

Materials and methods

In conventional cabinet drying system the hot drying air is thoroughly introduced at the bottom of the plenum chamber. The drying potential of the hot air is gradually diminished as it passes through the upper trays. In order to surmount the problem of non-uniformity in air flow pressure and temperature distributions in conventional cabinet dryers, a new version of cabinet dryer was designed and tested. In this design a side mounted plenum chamber with separate entries for each tray was added to the main structure of the dryer.

In order to find the most appropriate geometrical shape of cabinet dryer for achieving more uniform distribution of drying air flow inside the dryer, several geometries of air flow entries were investigated using the three dimensional CFD technique in the Fluent software. Finally geometry with the most uniform air flow pressure and temperature distribution in the dryer compartment was selected. The

width and laugh of the main body of the drying chamber were 45 and 60 cm respectively, Because one objective this study was comparison new design with amanlou and zomorodian design. The three dimensional shape of the dryer was made in the Gambit software. This structure was exported to Fluent software for investigating by CFD. The details of this new cabinet drying chamber are shown in Fig. 1 and Table 1.

Basic governing equations for designing the cabinet dryer

There are three categories of basic equations, which are derived from three basic laws of mass and energy conservation. The mass, momentum and energy conservation result in the continuity equation, Navier–Stokes equation and energy equation, respectively (Norton and Sun 2006). Reynolds number was calculated for different plans at the dryer entrance. In all cases Reynolds number was higher than 2000, thus the air flow showed a turbulent pattern inside the dryer (Fluent 6.3 user’s Guide 2005).

Several turbulent models were defined in commercial codes of CFD and it is left to the user to assert which one is appropriate for the case under his study (Norton and Sun 2006). Among turbulent models, the standard $k-\epsilon$ model still remains an industrial standard and its successful applications are reported in recent literature (Foster et al. 2005; Margaris and Ghiaus 2006).

The standard $k-\epsilon$ model is a semi-empirical model based on model transport equations for the turbulent kinetic energy (k) and its dissipation rate (ϵ). The transport equation for k is derived from the exact equation, while the transport equation for ϵ is obtained using physical reasoning and bears little resemblance to its mathematically exact counterpart (Yongson et al. 2007).

The turbulent kinetic energy, k , and its rate of dissipation, ϵ are obtained from the following transport equations:

$$\frac{\partial}{\partial t}(\rho k) + \frac{\partial}{\partial x_i}(\rho k u_i) = \frac{\partial}{\partial x_j} \left[\left(\mu + \frac{\mu_t}{\sigma_k} \right) \frac{\partial k}{\partial x_j} \right] + G_k + G_b - \rho \epsilon - Y_M + S_k \tag{1}$$

$$\frac{\partial}{\partial t}(\rho \epsilon) + \frac{\partial}{\partial x_i}(\rho \epsilon u_i) = \frac{\partial}{\partial x_j} \left[\left(\mu + \frac{\mu_t}{\sigma_\epsilon} \right) \frac{\partial \epsilon}{\partial x_j} \right] + C_{1\epsilon} \frac{\epsilon}{k} (G_k + C_{3\epsilon} G_b) - C_{2\epsilon} \rho \frac{\epsilon^2}{k} + S_\epsilon \tag{2}$$

Convective heat and mass transfer modeling in the $k-\epsilon$ models is given by the following equation (Yongson et al. 2007):

$$\left[\frac{\partial}{\partial t}(\rho E) + \frac{\partial}{\partial x_i} [u_i(\rho E + p)] \right] = \frac{\partial}{\partial x_i} \left[\left(k + \frac{c_p \mu_t}{Pr_t} \right) \frac{\partial T}{\partial x_i} + u_i(\tau_{ij})_{eff} \right] + S_h \tag{3}$$

Tray simulation

Fruit trays and aluminum net screen are porous media for air flow. Porous media are modeled by adding a momentum source term to the standard fluid flow equations. The source term is composed of two parts: a viscous loss term (the first term on the right-hand side of Eq. 4), and an inertial loss term (the second term on the right-hand side of Eq. 4) (Fluent 6.3 user’s Guide 2005).

$$S_i = - \left(\sum_{j=1}^3 D_{ij} \mu v_j + \sum_{j=1}^3 C_{ij} \frac{1}{2} \rho v_{mag} v_i \right) \tag{4}$$

Fig. 1 Details of the new cabinet dryer design: **a**: air inlet, **b**: vertical distance of the inlet, **c**: horizontal distance of the inlet, **d**: air inlet ducts, **e**: basements of the fruit holding trays, **k**: main air entries to the dryer, **f**: perforated screen, **l**: air exits from the dryer

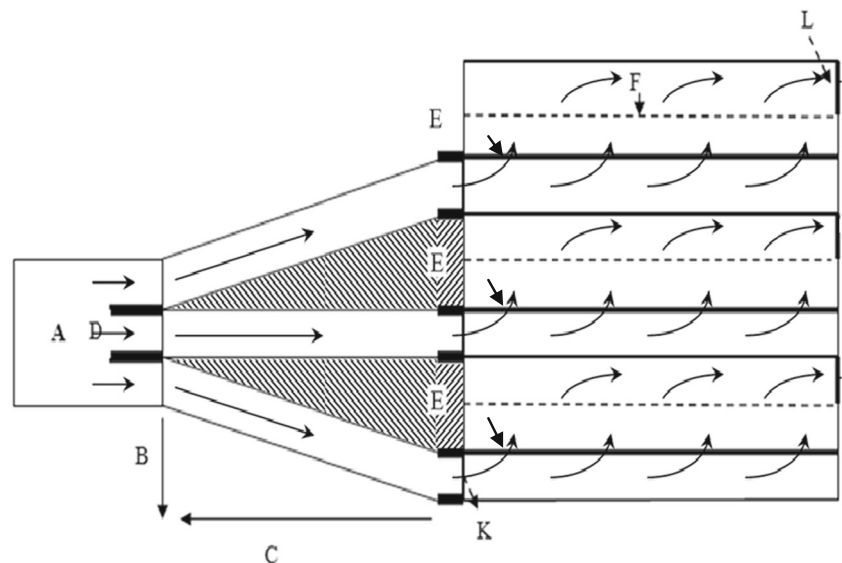


Table 1 Different locations in Fig. 2 and their proper dimensions, in cm

Locations	Proposed by Fluent	Best chosen by Fluent
A	Height 10–40 Length 10–30	Height 15 Length 25
B	0–40	15
C	15–60	30
D	0–20	10
E	5	5
F	Screen mesh no.= 8–15	Screen mesh no.= 12
K	05/15/13	8
L	03/10/13	6

Where S_i is the source term for the i th (x , y , or z) momentum equation and D & C are prescribed matrices. This momentum sink contributes to the pressure gradient in the porous cell, creating a pressure drop that is proportional to the fluid velocity (or velocity squared) in the cell.

Fluent 6.0.12 allows the source term to be modeled as a power law of the velocity magnitude:

$$S_i = -C_0|v|^{C_1} \quad (5)$$

Where C_0 and C_1 are user-defined empirical coefficients which are related to bed pressure drop of the porous media (Fluent 6.3 user's Guide 2005). In the present study for defining C_0 and C_1 , a test rig was designed and fabricated in which the pressure drop of drying fruit bed was measured. The test rig is made of a smooth PVC cylinder with 40 cm inside diameter. Air velocity and temperature can be adjusted and monitored in the test rig. The pressure drops across a thin layer (2.5–3 cm depth) of lemon fruit (84 % w.b initial moisture content) for random filling method were measured. Porosity of lemon bed was measured to be 45 %. The magnitude of C_0 and C_1 were also calculated to be 35.436 and 2.436 respectively.

Simulation details

In order to solve the governing equations, initial and boundary condition must be defined around the boundary of system (domain). Since the equations are generally nonlinear, they can not be solved by explicit method, closed-form analytical methods. The numerical finite volume method as proposed by Fluent 6.2 (Fluent 6: user's guide 2005) has been used for solving the equations on a PC P IV 3.2 GHz with 3 GB random access memory.

Double precision solver and segregated method were chosen. In this investigation the pattern of air flow during

drying process was important and since there was no variable condition in the study, the case was simulated as steady state condition.

Setting up of flow-simulating computation involves specific boundary conditions, in particular at surfaces bounding of the domain. In this study various boundary conditions were defined as followings:

- Inlet: three air velocities (1, 2 and 3, ms^{-1}) Direction of air flow was normal to air inlet.
- Outlet: assuming gauge pressure = 0 at the outlet, Fluent extrapolated the required information from the interior of drying chamber.
- Porous media: empirical parameters of pressure drop equation and fruit bed porosity and aluminum netting were defined.
- Wall: heat transfer coefficients of the chamber walls and environmental conditions were defined. Thermal conductivity, specific heat and density of the chamber wall were assumed to be: $0.16 \left(\frac{W}{m.K}\right)$, $1255 \left(\frac{J}{kg.K}\right)$ and $720 \left(\frac{kg}{m^3}\right)$ respectively (Incropera, and Dewitt. 1990). Ambient temperature and relative humidity were $15 \text{ }^\circ\text{C} \pm 1 \text{ }^\circ\text{C}$, and $30 \% \pm 2 \%$ respectively in all cases.

Experimental apparatus

The best design with the most uniform air temperature and air flow distribution for the drying chamber was chosen. In order to verify the CFD simulation results, this design was fabricated and evaluated under different operating conditions. Figure 2 shows the experimental layout of drying chamber and testing apparatus. A constant speed centrifugal fan (1400 rpm, 50 Hz, made in Italy) was used as an air flow source. An inverter (50 to 400 Hz, made in Japan) was inserted at the fan outlet to alter the air flow rate. The air flow was measured using a hot wire anemometer (Lutron, $\pm 0.1 \text{ m/s}$, made in Taiwan) located far enough from the fan outlet in a PVC pipe (15 cm ID.) connected to plenum chamber. Inlet air temperature to the drying bed was

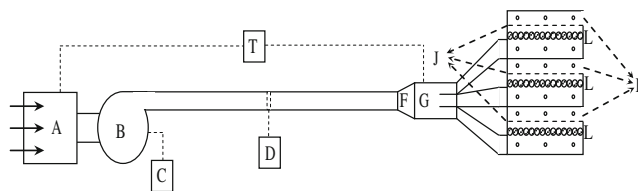


Fig. 2 Schematic diagram of the apparatus used in this research, **a** electrical heating unit, **b** centrifugal fan, **c** inverter, **d** hot wire anemometer, **t** thermostat, **f** diffuser, **g** air inlet, **e** air exist, **i** fruit trays, **j** aluminum netting

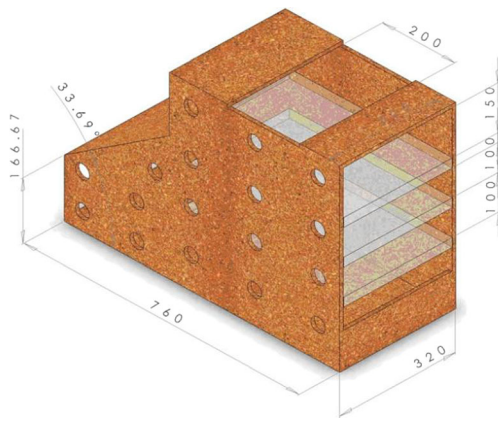


Fig. 3 cabinet drying chamber and the location of measurement points (Amanlou and Zomorodian 2010)

precisely controlled by a thermostatic sensor hanging just before the air was introduced into the dryer chamber (SAMWON, -50–150 °C, made in Korea). An electrical heating unit (6 kW) was attached to the fan inlet to regulate the air temperature introduced into the dryer.

These schemes enable us to simplify the simulation procedures and applying 3D CFD analysis for this study.

Lemon fruit (*Citrus Artifolia*) was chosen as a drying fruit and was randomly and uniformly spread on perforated stainless steel trays (3 cm in thickness). Three trays were tightly embedded in the drying chamber.

The best sketch was fabricated in the Department of Agricultural Engineering, Shiraz University, Shiraz, Iran. Chamber walls were made of pressed wood with the highest dimensional precision and all possible leaks were prevented. Experiments were carried out at three levels of inlet air velocity (1, 2, 3 ms⁻¹). Each experiment was replicated three times.

Amanlou and Zomorodian (2010) design a new cabinet dryer with a side mounted plenum chamber. To approach a uniform distribution of drying air flow and temperature taking into account the overall operating conditions, seven different geometries of cabinet dryer were envisaged. Air inlet and exit size and their locations, distance of fruit trays from dryer ceilings, angle of side plenum chamber with respect to horizon, effect of hood type air exit and effect of introducing a deflector into the air inlet were important parameters which were considered and evaluated in the different designs. In order to find the best uniform air flow and temperature distribution in the drying chamber theoretically, three dimensional CFD was employed using fluent software, Fig. 3.

Data acquisition procedures

For measuring the air velocity and temperature during each test, at different locations inside the drying chamber, 18 points on the side wall of the drying chamber (under and over of the screen holding material) were pierced. All holes except the one through which hot wire probe was inserted for air velocity measurement, were filled tightly by conic plastic washers. Inlet air temperature and velocity were kept constant in each set of experiment. For reading air temperature and velocity at each point (three points under and three points over the screens) inside the drying cabinet, hot wire probe was inserted through the hole and adjusted at three different equidistant locations along the depth of the drying chamber. The average of three readings with three replications was selected as the experimental data for a single point. The corresponding values of air temperature and velocity of 18 holes extracted from

Fig. 4 Air velocity distribution profiles for the new cabinet dryer at inlet air velocity of 1 ms⁻¹

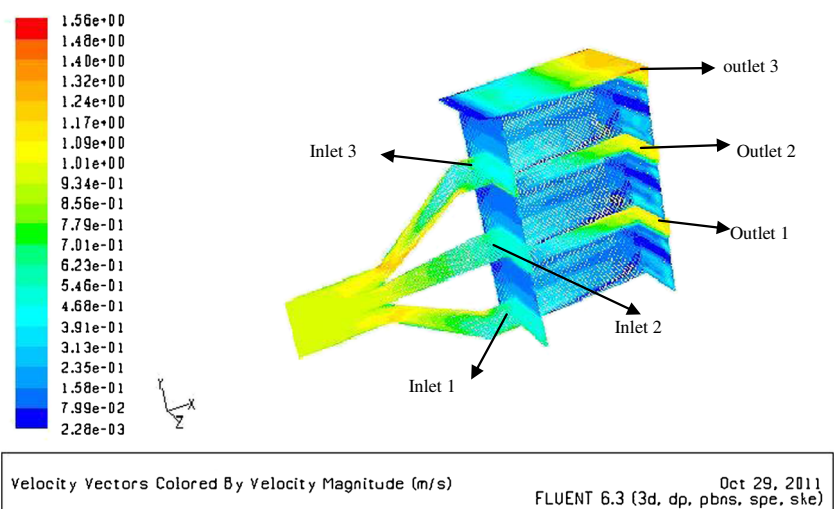
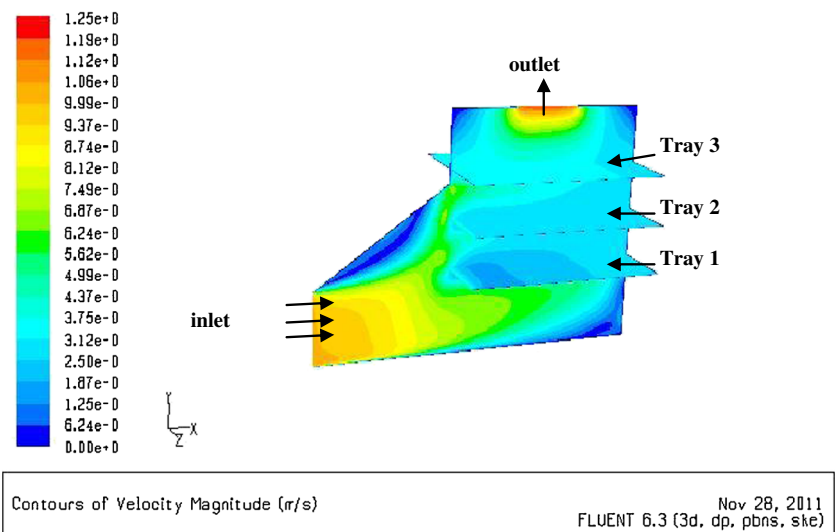


Fig. 5 Air velocity distribution profiles for the existing cabinet dryer at inlet air velocity of 1 ms^{-1}



the 3d CFD analysis were compared with the experimental data.

Results and discussions

To decide about the suitability of the design of the new cabinet dryer and comparison with existing dryer data analysis of different proposed plans were carried out using three dimensional CFD. The most feasible design can be assessed by comparing the uniformity of air flow distribution in the drying chamber as done by many other researchers (Mulet et al. 1987; Karathanos and Belessiotis 1997; Mathioulakis et al. 1998; Amanlou and Zomorodian 2010).

The velocity distribution profiles for the new design are shown in Fig. 4, and for existing cabinet dryer shown in Fig. 5.

The profile showed in Fig. 4, a very uniform air flow distribution in the three entries of the drying air channel beneath the perforated holding material screens as well as the above of the screens. This proved that the main goal of the research has been achieved. But the profile showed in Fig. 4, air distribution in the tray 1 more than tray 2 and tray 3.

The experimental results collected from 18 points inside the drying compartment for velocity were compared with the corresponding results extracted from the CFD analysis for tow dryers. The results of statistical comparison illustrated very good correlation between the predicted CFD and

Fig. 6 The experimental moisture content of the drying fruits on each tray in the new dryer

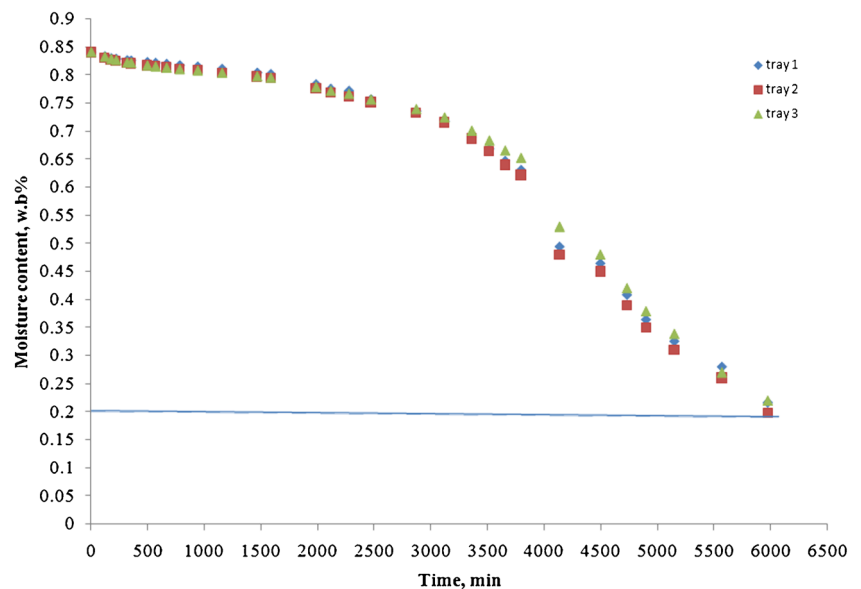
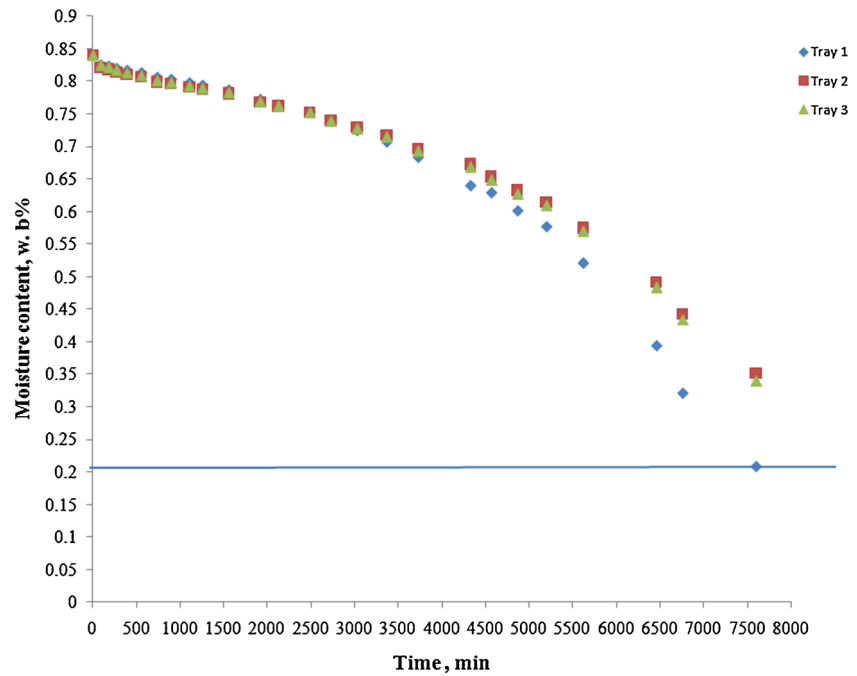


Fig. 7 The experimental moisture content of the drying fruits on each tray in the Amanlou and Zomorodian dryer's



experimental data. Indeed knowing the physical properties of drying fruit (pressure drop and porosity), the $k-\epsilon$ model was a very powerful tool for investigating the air velocity distribution patterns inside the drying chamber. Adding a porous media term to momentum equation, would help to a true simulation of the cabinet drying chamber.

Furthermore, for proving a uniform air flux and simultaneous drying process for the drying products on the three trays, the lemon moisture content of randomly pickup kernels on each tray were measured during the drying time. The moisture contents of the fruits on each tray were plotted versus the drying elapse time, Figs. 6 and 7.

The initial and final moisture contents of the lemon kernels were 84 % (wb) and 20 % (wb) respectively. Statistical analysis showed no significant difference between the moisture content of different kernels on different trays after 6000 min of drying time. But in the amanlou and zomorodian dryer's after 7900 min of drying time tray 1 was reached moisture content 20 % and tray 2 and tray3 have 35 % and 33 % moisture content respectively.

Conclusions

- 3-dimensional Computational Fluid Dynamic (CFD) was a very powerful tool for the cabinet dryer system analysis.
- The standard $k-\epsilon$ model using empirical data (fruit trays pressure drop and porosity) showed very accurate results.

- Aluminum netting above the trays had a good effect in the uniform air velocity in the fruit trays.
- Comparing the experimental and predicted data (extracted for the CFD analysis) revealed a very good correlation coefficient of 0.99 for drying air velocity in the drying chamber.
- comparison the new cabinet dryer with the existing design (Amanlou and Zomorodian 2010) showed the new design was superior to the existing design in all of aspects.

References

Amanlou Y, Zomorodian A (2010) Applying CFD for designing a new fruit cabinet dryer. J Food Eng 101:8–15

Adams RL, Thompson JF (1985) Improving drying uniformity in concurrent flow tunnel dehydrators. Trans ASAE 28(3):890–892

Anderson JD (1995) Computational fluid dynamics. International Edition. McGraw-Hill, New York

Fluent 6.3 user's Guide (2005) Fluent documentation. Fluent Inc, Lebanon

Foster AM, Madge M, Evans JA (2005) The use of CFD to improve the performance of a chilled multi-deck retail display cabinet. Int J Refrig 28:698–705

Franco ADL, Valeva A, Pena A, Perez M (2011) Aerodynamic and lysis CFD simulation of several cellulose evaporative cooling pads used in Mediterranean greenhouses. 76: 218–230

Hong SI, Lee H, Hwang I, Seo J, Bitog J, Song (2011) CFD modeling of livestock odour dispersion over complex terrain. 108: 253–264

- Incropera FP, DeWitt DP (1990) Fundamentals of heat and mass transfer. Wiley, New York
- Karathanos VT, Belessiotis VG (1997) Sun and artificial air drying kinetics of some agricultural products. *J Food Eng* 31(1):35–46
- Margaris DP, Ghiaus AG (2006) Dried product quality improvement by air flow manipulation in tray dryers. *J Food Eng* 75:542–550
- Mathioulakis E, Karathanos VT, Belessiotis VG (1998) Simulation of air movement in a dryer by computational fluid dynamics: application for the drying of fruits. *J Food Eng* 36:183–200
- Mirade PS (2003) Prediction of the air velocity field in modern meat dryers using unsteady computational fluid dynamics (CFD) models. *J Food Eng* 60:41–48
- Mulet A, Berna A, Borrás M, Pinaga F (1987) Effect of air flow rate on carrot drying. *Dry Technol* 5(2):245–258
- Norton T, Sun DW (2006) Computational fluid dynamics (CFD)—an effective and efficient design and analysis tool for the food industry: a review. *Trends Food Sci Technol* 17:600–620
- Norton T, Grant J, Fallon R, Sun D (2010) Improving the representation of thermal boundary conditions of livestock during CFD modeling of the indoor environment. *Journal of Computers and Electronics in Agriculture* 73:17–36
- Scott G, Richardson P (1997) The application of computational fluid dynamics in the food industry. *Trends Food Sci Technol* 8:119–124
- Verboven P, Scheerlinck N, De Baerdemaeker J, Nicolai BM (2000a) Computational fluid dynamics modeling and validation of the temperature distribution in a forced convection oven. *J Food Eng* 43:61–73
- Verboven P, Scheerlinck N, De Baerdemaeker J, Nicolai BM (2000b) Computational fluid dynamics modeling and validation of the isothermal airflow in a forced convection oven. *J Food Eng* 43:41–53
- Xia B, Sun DW (2002) Applications of computational fluid dynamics (CFD) in the food industry: a review. In: Sun DW (ed), *CFD Applications in the Agri-Food Industry* (special issue) *Computers and Electronics in Agriculture*, 34(1–3): 5–24
- Yongson O, Badruddin IA, Zainal ZA, Narayana PAA (2007) Airflow analysis in an air conditioning room. *Build Environ* 42:1531–1537